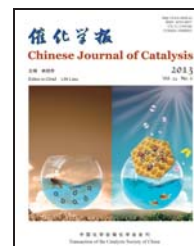




available at www.sciencedirect.com



journal homepage: www.elsevier.com/locate/chnjc



## Article

# Pd nanoparticles confined in fluoro-functionalized yolk-shell-structured silica for olefin hydrogenation in water

LI Xiaofei <sup>a,b</sup>, ZHANG Wenjuan <sup>b</sup>, ZHANG Limin <sup>a,\*</sup>, YANG Hengquan <sup>b,#</sup><sup>a</sup> School of Chemistry and Materials Science, Shanxi Normal University, Linfen 041000, Shanxi, China<sup>b</sup> School of Chemistry and Chemical Engineering, Shanxi University, Taiyuan 030006, Shanxi, China

## ARTICLE INFO

## Article history:

Received 24 December 2012

Accepted 5 March 2013

Published 20 June 2013

## Keywords:

Palladium

Functionalization

Olefin

Aqueous phase

Hydrogenation

## ABSTRACT

Pd nanoparticles were confined in yolk-shell mesoporous silica via encapsulation, etching and modification, producing a functionalized yolk-shell-structured catalyst. This catalyst was characterized using X-ray diffraction analysis, transmission electron microscopy, N<sub>2</sub> adsorption-desorption, and thermogravimetric analysis. The catalyst had high activity for olefin hydrogenation in water, higher than that of the unmodified counterpart. The catalyst can be recovered through centrifugation, and its activity is not significantly decreased after several reaction cycles.

© 2013, Dalian Institute of Chemical Physics, Chinese Academy of Sciences.

Published by Elsevier B.V. All rights reserved.

## 1. Introduction

Recently, using water as a medium in catalytic reactions has attracted extensive attentions because of it is low-cost, safe, and pollution-free [1–6]. However, because of its low solubility in water, most organic reactants cannot completely contact with the catalyst, which leads to low conversion in catalytic reactions. The addition of co-solvent or surfactants can improve the reaction rate [7,8], but introduction of auxiliary additives violates the green chemistry principles. It is also difficult to separate and purify the products. Therefore, development of a highly active catalyst for water-mediated systems is still a challenge.

Yolk-shell microspheres have emerged as a rapidly growing catalysis research theme because of their unique structure [9–20], compared with conventional structures, such as MCM-41 and SBA-15. First, yolk-shell microspheres have a

special hollow structure and low density, which are conducive to the catalyst suspension in water. The reactants also diffuse quickly to the surface of the catalyst because of the hollow structure, which can further improve the reaction rate [21,22]. Second, yolk-shell microspheres have interstitial space between the shell and the core, which can enrich more reactants and provide greater possibility for effective reactants to interact with the catalyst. Third, the outer shell can hinder the aggregation of neighboring particles, which enhances their stability [23].

Catalytic performance can be improved by increasing the hydrophobicity of the catalysts. Yang and co-workers [24] found that organically functionalized mesoporous materials exhibit significantly enhanced hydrothermal and mechanical stability. Hydrophobic mesoporous materials can also increase the adsorption of hydrophobic pollutants in aqueous solutions [25,26]. Therefore, catalyst hydrophobization can exhibit sig-

\* Corresponding author. Tel: +86-13663578554; E-mail: zhangliminsxu@gmail.com

# Corresponding author. Tel: +86-13643472170; E-mail: hqyang@sxu.edu.cn

This work was supported by the National Natural Science Foundation of China (20903065 and 21173137).

DOI: 10.1016/S1872-2067(12)60561-0 | http://www.sciencedirect.com/science/journal/18722067 | Chin. J. Catal., Vol. 34, No. 6, June 2013

nificantly enhanced activity in aqueous environments [27,28]. However, much higher hydrophobicity of the catalyst can hinder effective interactions with the reactants, which leads to low catalyst activity.

The fluoropropyl group is a moderately hydrophobic functional group. Fluoro-functionalized solid catalysts are hydrophobic, causing increased adsorption of the reactants [29,30], and leading to an enhanced reaction rate. Until recently, little attention had been paid to the preparation of the fluoropropyl-functionalized yolk-shell structured catalysts and their catalytic performance in water systems.

In this work, we report the synthesis of fluoro-functionalized yolk-shell silica with Pd nanoparticles cores (yPd@mSiO<sub>2</sub>-F) via impregnation-reduction, encapsulation, etching and grafting. The structure and composition of the samples were characterized with X-ray diffraction (XRD), transmission electron microscope (TEM), N<sub>2</sub> adsorption-desorption, and thermal gravimetric analysis (TGA). The catalytic reactivity and recycling performance were studied through hydrogenation in water.

## 2. Experimental

### 2.1. Preparation of catalyst

Deionized water (20 ml) and ammonia solution (12.2 ml, 25%) were added to 200 ml of absolute ethanol. After vigorous stirring for 30 min, 12.4 ml of tetraethylorthosilicate (TEOS) was slowly added. After further stirring for 12 h, aqueous-phase dispersed silica nanospheres were generated. The silica nanospheres (SiO<sub>2</sub>) [31] were obtained by filtration, purification with deionized water and drying at room temperature.

The prepared SiO<sub>2</sub> (0.8 g) was added to 10 ml of toluene containing 0.0084 g of Pd(OAc)<sub>2</sub>. After stirring for 4 h at room temperature, the toluene was removed by centrifugation to obtain the Pd-adsorbed solid. The solid was then reduced with NaBH<sub>4</sub> in 16 ml of toluene and ethanol (V/V = 20:1). This solid was separated by centrifugation and washed with ethanol. After vacuum drying, Pd/SiO<sub>2</sub> was obtained.

The prepared Pd/SiO<sub>2</sub> (0.6 g) was dispersed into 120 ml of H<sub>2</sub>O using ultrasound. Cetyltrimethylammonium bromide (CTAB) solution containing 0.9 g CTAB, 180 ml water, 180 ml ethanol, and 3.3 ml ammonia solution (25%) were slowly added under stirring. TEOS (1.0575 g) was successively added to the solution under stirring. After centrifugation, the materials were added to 120 ml of deionized water and uniformly dispersed under ultrasonic. Sodium carbonate (2.544 g) was added for etching at 50 °C for 12 h under N<sub>2</sub> atmosphere. The final product was denoted as yPd@mSiO<sub>2</sub>.

To synthesize the yolk-shell yPd@mSiO<sub>2</sub>-F, 0.5 g of yPd@mSiO<sub>2</sub> and 0.1635 g of 3,3,3-trifluoropropyltrimethoxysilane were added to 5 ml of toluene solution and refluxed for 4 h under a N<sub>2</sub> atmosphere at 100 °C. The final material denoted as yPd@mSiO<sub>2</sub>-F was prepared by centrifugation and washed with toluene and ethanol.

### 2.2. Characterization

TEM was performed using a JEM-2000EX (JEOL, Japan, Aki-shima) at an acceleration voltage of 120 kV. Nitrogen sorption isotherms were measured at -196 °C with an ASAP2020 volumetric adsorption analyzer. The BET surface area was calculated from the adsorption data in the relative pressure range  $p/p_0$  from 0.05 to 0.3. Pore size distribution was determined from the desorption branch of the isotherm using the BJH method. Pore volume was estimated at a relative pressure  $p/p_0$  of 0.995. XRD patterns were recorded on a Rigaku D/max-2400 X-ray diffractometer (at 40 kV and 100 mA of Cu K<sub>α</sub> radiation). TGA was performed with a NETZSCH TG analyzer (Germany) under nitrogen from room temperature to 900 °C with a heating rate of 25 °C/min.

### 2.3. Hydrogenation of olefin

For hydrogenation of olefin, the catalytic experiment was carried out in a three-necked flask fitted with water bath, thermocouple, and magnetic stirrer. A mixture of H<sub>2</sub>O (6 ml), substrate (1 mmol), and catalyst (0.1 mol %) was prepared in the three-necked flask. After air was flushed out of the reactor, bath was heated to reaction temperature and then was pressurized with H<sub>2</sub> to 0.15 MPa. Then the mixture was stirred at 500 r/min and the reaction was considered to start. After the reaction, the catalyst was removed from the reaction mixture by centrifugation; the products were analyzed by gas chromatography (Agilent 7890A) with a flame ionization detector.

## 3. Results and discussion

### 3.1. Catalyst preparation and characterization

The typical procedure for the preparation of yolk-shell yPd@mSiO<sub>2</sub> is outlined in Fig. 1. To confine the Pd nanoparticles to the interior of the yolk-shell, we loaded the Pd nanoparticles on SiO<sub>2</sub> spheres through dipping and reduction, and grew a silica shell on its surface in the presence of CTAB, then etched the SiO<sub>2</sub> core with Na<sub>2</sub>CO<sub>3</sub>. A yolk-shell-structure catalyst was obtained after removing the template by solvent extraction. A previous method mentioned in the literature obtains a hollow structure using high temperature calcination to remove the carbon sphere [32]. Our preparation is implemented under milder conditions, which avoids the collapse of structure and deactivation of the active component that may be caused by

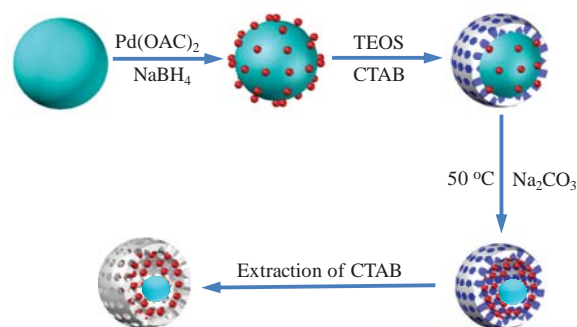
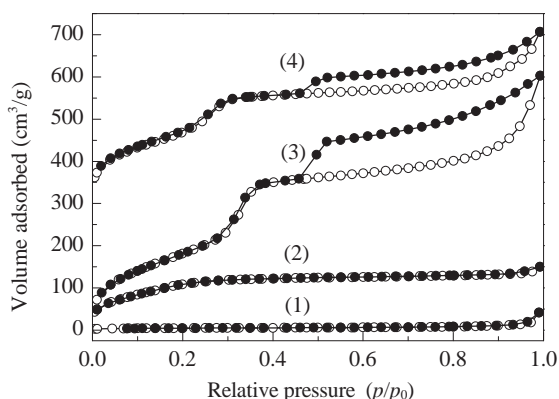


Fig. 1. Illustration of the synthesis procedure for the yolk-shell yPd@mSiO<sub>2</sub>.



**Fig. 2.** N<sub>2</sub> adsorption-desorption isotherms of SiO<sub>2</sub> (1), Pd/SiO<sub>2</sub>@mSiO<sub>2</sub> (2), yPd@mSiO<sub>2</sub> (3), and yPd@mSiO<sub>2</sub>-F (4). yPd@mSiO<sub>2</sub> is offset vertically by 300; yPd@mSiO<sub>2</sub>-F is offset vertically by 50.

calculation under high temperature.

The structures of the synthesized materials were characterized by N<sub>2</sub> sorption. N<sub>2</sub> sorption isotherms are displayed in Fig. 2, and the parameters are summarized in Table 1. The N<sub>2</sub> adsorption amount of SiO<sub>2</sub> was very small in the entire pressure ranges, with a surface area of only 18 m<sup>2</sup>/g and pore volume of 0.06 cm<sup>3</sup>/g. Pd/SiO<sub>2</sub>@mSiO<sub>2</sub> was achieved after encapsulating Pd/SiO<sub>2</sub> with SiO<sub>2</sub>, showing a type IV sorption isotherm. The capillary condensation steps were shown in the relative pressure range of 0.1–0.3. The data show that specific surface area increased to 408 m<sup>2</sup>/g and the pore volume increased to 0.23 cm<sup>3</sup>/g, which is due to the formation of the porous structure on the Pd/SiO<sub>2</sub> surface. The adsorption isotherm of yPd@mSiO<sub>2</sub> was also close to type IV. The capillary condensation steps were shown in the relative pressure range of 0.3–0.5, indicating that a mesoporous structure had formed. In addition, there was no overlap between the yPd@mSiO<sub>2</sub> adsorption branch and the desorption branch in the relative pressure range of 0.5–1.0. A clear H4 type hysteresis loop proved that the material had a hollow structure. In comparison to Pd/SiO<sub>2</sub>@mSiO<sub>2</sub>, the specific surface area and pore volume of yPd@mSiO<sub>2</sub> increased, respectively, to 841 m<sup>2</sup>/g and 1.01 cm<sup>3</sup>/g. This was mainly because the SiO<sub>2</sub> cores were etched away, and the template had been fully removed. There was no significant difference between the yPd@mSiO<sub>2</sub> adsorption branch and the yPd@mSiO<sub>2</sub> desorption branch, but the specific surface area, pore volume

**Table 1**

Texture properties of the samples.

Sample	$A_{\text{BET}}/(\text{m}^2/\text{g})$	$V^a/(\text{cm}^3/\text{g})$	Pore size <sup>b</sup> (nm)
SiO <sub>2</sub>	18	0.06	—
Pd/SiO <sub>2</sub> @mSiO <sub>2</sub>	408	0.23	1.90
yPd@mSiO <sub>2</sub>	841	1.01	2.85
yPd@mSiO <sub>2</sub> -F	619	0.63	2.40

<sup>a</sup> Single point pore volume calculated at relative pressure  $p/p_0$  of 0.99.

<sup>b</sup> BJH method from adsorption branch.

and pore size were significantly reduced, indicating that the fluoropropyl groups were successfully grafted onto yPd@mSiO<sub>2</sub>.

Typical TEM images of SiO<sub>2</sub> and yPd@mSiO<sub>2</sub> are shown in Fig. 3. The obtained SiO<sub>2</sub>, with an average particle size of 200 nm, is shown in Fig. 3(a). For the Pd/SiO<sub>2</sub> sample, Pd nanoparticles sizes are uniformly distributed over a range of 4–10 nm. After encapsulation, etching and modification, uniform and nearly monodisperse yolk-shell yPd@mSiO<sub>2</sub> (Fig. 3(c)) with an average particle size of 500 nm were obtained. The size of the microspheres was significantly greater than SiO<sub>2</sub>.

The XRD patterns of yPd@mSiO<sub>2</sub> and yPd@mSiO<sub>2</sub>-F are shown in Fig. 4. The XRD patterns of yPd@mSiO<sub>2</sub> are similar to yPd@mSiO<sub>2</sub>-F, showing one diffraction peak at  $2\theta \approx 2.3^\circ$  of similar intensity. The XRD and TEM results suggest that the yolk-shell-structured silica still possesses a mesoporous shell.

The TG plots for yPd@mSiO<sub>2</sub> and yPd@mSiO<sub>2</sub>-F are shown in Fig. 5. TG curves reveal that three stages of decomposition

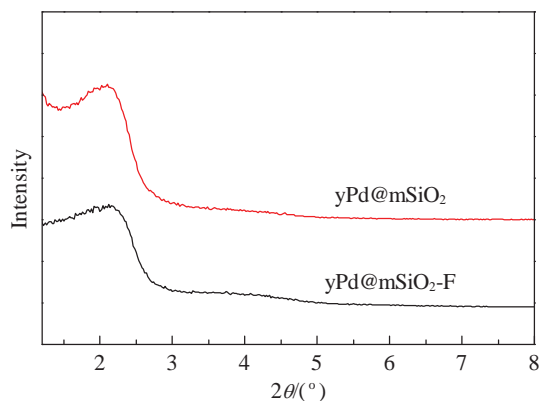


**Fig. 4.** XRD patterns of yPd@mSiO<sub>2</sub> and yPd@mSiO<sub>2</sub>-F samples.

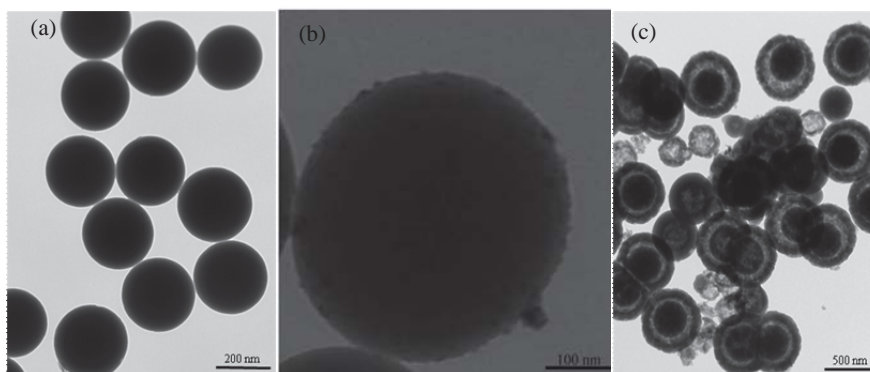


**Fig. 3.** TEM images of SiO<sub>2</sub> (a), Pd/SiO<sub>2</sub> (b), and yPd@mSiO<sub>2</sub> (c).

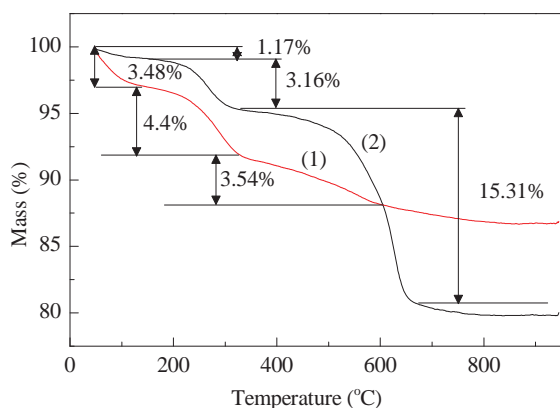


Fig. 5. TGA curves of yPd@mSiO<sub>2</sub> (1) and yPd@mSiO<sub>2</sub>-F (2) samples.

occur for yPd@mSiO<sub>2</sub>. Similar results have been found for yPd@mSiO<sub>2</sub>-F. Stage 1 is from the start temperature (50 °C) to 200 °C, stage 2 is from 200 to 320 °C, and the third stage is from 320 to 900 °C. In stage 1, yPd@mSiO<sub>2</sub> experiences about 3.48% weight loss mainly due to the elimination of the physically adsorbed water, but yPd@mSiO<sub>2</sub>-F only undergoes 1.17% of weight loss. This is mainly due to the introduction of fluoropropyl, causing an increase in the hydrophobicity of the surface of the material and reducing the adsorption quantity of water. In stage 2, there is a 4.4% weight loss for yPd@mSiO<sub>2</sub>, and 3.16% for yPd@mSiO<sub>2</sub>-F, where most of the template is released. Most of the weight loss that takes place in stage 3 is due to the elimination of condensation dehydration of the silica groups. In this stage, there can be up to 15.31% weight loss for yPd@mSiO<sub>2</sub>-F, and higher than 3.54% for yPd@mSiO<sub>2</sub>. This is mainly due to the decomposition of grafted fluoropropyl group and the condensation dehydration of silica groups at high temperatures. According to the TG results, we can calculate the loading of fluoropropyl to be about 1.2 mmol/g, which is consistent with the results of elemental analysis.

### 3.2. Catalytic activity of the catalysts

Many studies [33–35] have been conducted concerning the hydrogenation of olefin in aqueous media because of its importance in industrial fields. This paper looks at hydrogenation in water to evaluate the catalytic activity of yolk-shell structure materials. yPd@mSiO<sub>2</sub>-F and yPd@mSiO<sub>2</sub> were used in the hydrogenation of methyl acrylate, and the reaction rate monitored by recording the H<sub>2</sub> pressure with the results shown in Fig. 6. Under the same conditions, the consumption of hydrogen on the yPd@mSiO<sub>2</sub>-F is significantly faster than on the yPd@mSiO<sub>2</sub>. This demonstrates that the activity of yPd@mSiO<sub>2</sub>-F is much higher than yPd@mSiO<sub>2</sub>. For the ethyl methacrylate, similar results were obtained, as shown in Fig. 7. The hydrogen consumption rate of the above two substrates proves that yPd@mSiO<sub>2</sub>-F has a higher catalytic activity.

Hydrogenation of several typical olefins under aqueous conditions was further explored. Hydrogenation of all the olefins proceeded efficiently and quantitative yields were almost achieved (Table 2). Of all the olefins, styrene, with the smallest

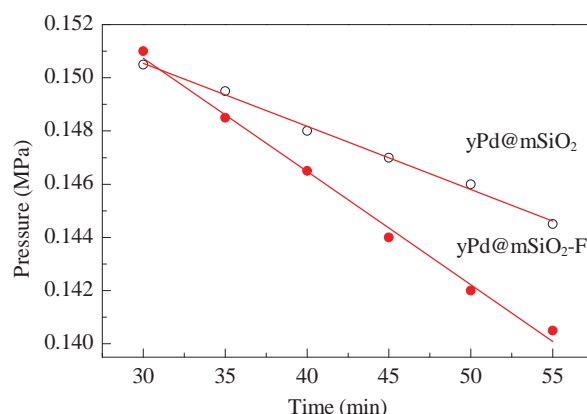


Fig. 6. The reaction kinetics of hydrogenation of methyl acrylate over the two catalysts in pure water. Reaction conditions: substrate 2 mmol, water 6 ml, 0.15 MPa, 0.1% Pd, 30 °C, fixed stirring rate.

polarity smallest afforded conversions of 45% with yPd@mSiO<sub>2</sub> and 88% with yPd@mSiO<sub>2</sub>-F within 45 min. For aliphatic olefins, butyl acrylate, butyl methacrylate, methyl acrylate, and ethyl methacrylate, the conversion rate on yPd@mSiO<sub>2</sub>-F was much higher than on yPd@mSiO<sub>2</sub> under the same conditions. For acrylamide, yPd@mSiO<sub>2</sub> offered a 49% conversion within 60 min, and yPd@mSiO<sub>2</sub>-F offered 99%, where the latter is much higher than the former. The results further confirm that yPd@mSiO<sub>2</sub>-F shows higher activity than yPd@mSiO<sub>2</sub> for the hydrogenations of olefins. This is because the shell of yPd@mSiO<sub>2</sub> was modified by fluoropropyl, and exhibited moderate hydrophobicity. This drives the organic reactants into the intracavity of the yolk-shell, promoting sufficient contact of the reactant and the Pd nanoparticles, leading to an improved reaction rate.

### 3.3. Catalyst recycling

The reusability of catalysts is very important theme and makes them useful for commercial applications. Thus, the recovery and reusability of yPd@mSiO<sub>2</sub>-F has been investigated using butyl acrylate as a model substrate. The results are tabu-

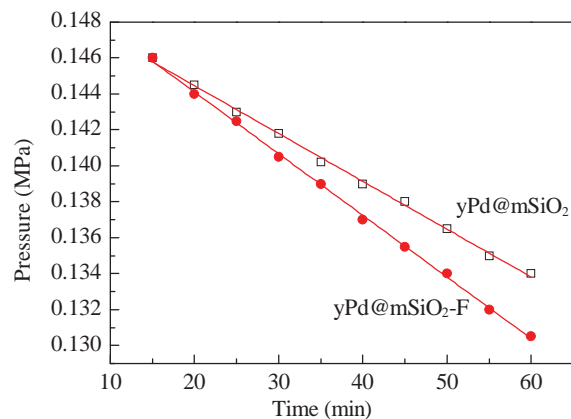
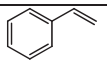
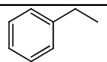
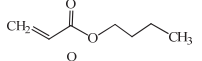
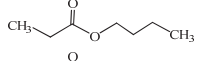
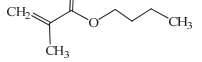
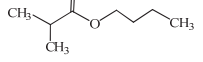
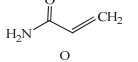
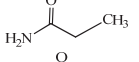
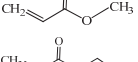
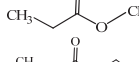
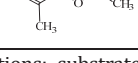
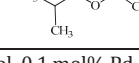


Fig. 7. The reaction kinetics of hydrogenation of ethyl methacrylate over the two catalysts in pure water. Reaction conditions: substrate 2 mmol, water 6 ml, 0.15 MPa, 0.1% Pd, 25 °C, fixed stirring rate.

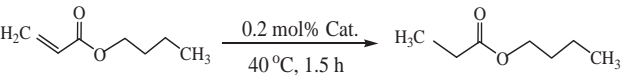


**Table 2**

Results of hydrogenation of different substrates over the two catalysts.

Entry	Substrate	Product	Time (min)	Temperature (°C)	Pressure (MPa)	Conversion <sup>a</sup> (%)	
						yPd@mSiO <sub>2</sub>	yPd@mSiO <sub>2</sub> -F
1			45	25	0.15	45	88
2			30	30	0.15	48	96
3			60	50	0.30	79	92
4			60	35	0.15	49	99
5			45	30	0.15	65	94
6			60	25	0.15	71	94

Reaction conditions: substrate 1 mmol, 0.1 mol% Pd, H<sub>2</sub>O 6 ml. <sup>a</sup>Determined by GC**Table 3**Recycling results of yPd@mSiO<sub>2</sub>-F.

	
Cycle	Conversion* (%)
1	99
2	99
3	98
4	99
5	99

Reaction conditions: substrate 1 mmol, 0.2% Pd, water 3 ml, 40 °C, 1.5 h, ambient H<sub>2</sub> pressure. \*Determined by GC.

lated in Table 3. The catalyst is highly reusable, retaining its catalytic activity over five reaction cycles. The conversion rate was about 98% for every cycle within the same time.

To ascertain whether the catalyst was truly heterogeneous, or whether it acts as a reservoir for active soluble Pd, a filtration test was performed. In a typical experiment, Pd complex (0.1 mol%), acrylamide (2 mmol), and H<sub>2</sub>O (6 ml) were taken in a round-bottomed flask and stirred at 35 °C for 30 min. At this stage (52% conversion), the catalyst was filtered off and the experiment continued with the filtrate for another 30 min. There was no detectable increase in the product concentration. The conversion was 54%, which was significantly lower than a 99% conversion over yPd@mSiO<sub>2</sub>-F within the same time. These results can confirm the heterogeneous character of the catalytically active species. To verify the stability of the catalyst, the structure of the catalyst after five uses was analyzed with N<sub>2</sub> adsorption-desorption. The data show that the specific surface area is 382 m<sup>2</sup>/g and the pore volume is 0.23 cm<sup>3</sup>/g, which is a little lower than those of the fresh catalyst. This demonstrates good stability of the developed catalyst.

#### 4. Conclusions

In conclusion, a new Pd catalyst based on fluoro-functionalized yolk-shell-structured silica (yPd@mSiO<sub>2</sub>-F) was prepared and applied in olefin hydrogenation. Characteri-

zations show that the catalyst has a high specific area, and that its shell has uniformly distributed mesoporous channels. yPd@mSiO<sub>2</sub>-F show higher catalytic activity than yPd@mSiO<sub>2</sub> for the hydrogenation of olefin. This is because the shell of yPd@mSiO<sub>2</sub> modified by fluoropropyl exhibits moderate hydrophobicity, which can drive the organic reactants into the intracavity of the yolk-shell. This promotes sufficient contact of the reactant and Pd nanoparticles, leading to high reaction rates. The activity of yPd@mSiO<sub>2</sub>-F did not significantly decrease after five reaction cycles, and the catalyst showed good stability. Our research preliminarily demonstrates that the unique structure and easy functionalization features make the yolk-shell-structured catalyst promising for more aqueous reactions.

#### References

- Wang J B, Qin R X, Xiong W, Jia Y, Liu D R, Feng J, Chen H. *Chin J Catal* (王金波, 秦瑞香, 熊伟, 贾云, 刘德蓉, 冯建, 陈华. 催化学报), 2010, 31: 273
- Zhang Y, Wang M X, Wang D, Huang Z T. *Progr Chem* (张岩, 王梅祥, 王东, 黄志铿. 化学进展), 1999, 11: 394
- Yang H Q, Jiao X, Li Sh R. *Chem Commun*, 2012, 48: 11217
- Ma Zh Ch, Yang H Q, Qin Y, Hao Y J, Li G. *J Mol Catal A*, 2010, 331: 78
- Datta B, Pasha M A. *Ultrasonics Sonochem*, 2013, 20: 303
- Lu A, Cotanda P, Patterson J P, Longbottom D A, O'Reilly R K. *Chem Commun*, 2012, 48: 9699
- Xu X, Ji F Y, H L. *J Civil Arch Envir Eng* (徐璇, 吉芳英, 何莉. 土木建筑与环境工程), 2011, 33: 129
- Kong F Z, Tian J H, Jin Z L. *Petro Technol* (孔凡志, 田建华, 金子林. 石油化工), 2002, 31: 387
- Huang L H, Chen C X, Liu Y L. *Chin J Catal* (黄浪欢, 陈彩选, 刘应亮. 催化学报), 2006, 27: 1101
- Lin Y S, Wu S H, Tseng C T, Hung Y, Chang C, Mou C Y. *Chem Commun*, 2009: 3542
- Lee I, Albitzer M A, Zhang Q, Ge J P, Yin Y D, Zaera F. *Phys Chem Chem Phys*, 2011, 13: 2449
- Guan Zh H, Hu J L, Gu Y L, Zhang H J, Li G X, Li T. *Green Chem*, 2012, 14: 1964
- Kim M, Park J C, Kim A, Park K H, Song H. *Langmuir*, 2012, 28:

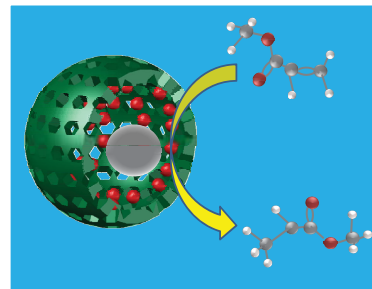
## Graphical Abstract

Chin. J. Catal., 2013, 34: 1192–1200 doi: 10.1016/S1872-2067(12)60561-0

**Pd nanoparticles confined in fluoro-functionized yolk-shell-structured silica for olefin hydrogenation in water**

Li Xiaofei, ZHANG Wenjuan, ZHANG Limin\*, YANG Hengquan\*  
Shanxi Normal University; Shanxi University

The fluoro-functionized yolk-shell-structured catalyst (yPd@mSiO<sub>2</sub>-F) exhibited higher activity than the non-functionized catalyst (yPd@mSiO<sub>2</sub>) in the hydrogenation of olefins in water.



- 6441
- [14] Fang X L, Liu Zh H, Hsieh M F, Chen M, Liu P X, Chen Ch, Zheng N F. *ACS Nano*, 2012, 6: 4434
- [15] Wang Y L, Wang F Y K, Chen B D, Xu H, Shi D L. *Chem Commun*, 2011, 47: 10350
- [16] Sun H, Shen X Sh, Yao L, Xing Sh X, Wang H, Feng Y H, Chen H Y. *J Am Chem Soc*, 2012, 134: 11243
- [17] Kuo Ch H, Tang Y, Chou L Y, Sneed B T, Brodsky C N, Zhao Z P, Tsung C K. *J Am Chem Soc*, 2012, 134: 14345
- [18] Wang F Y K, Tang Y L, Zhang B B, Chen B D, Wang Y L. *J Colloid Interf Sci*, 2012, 386: 129
- [19] Wang P, Bai S Y, Li B, Yang Q H. *Chin J Catal* (王鹏, 白诗扬, 李博, 杨启华. 催化学报), 2012, 33: 1689
- [20] Li X B, Yang Y, Yang Q H. *J Mater Chem A*, 2013, 1: 1525
- [21] Yang Y, Liu J, Li X B, Liu X, Yang Q H. *Chem Mater*, 2011, 23: 3676
- [22] Chen H M, Liu R S, Lo M Y, Chang S C, Tsai L D, Peng Y M, Lee J F. *J Phys Chem C*, 2008, 112: 7522
- [23] Tan L F, Chen D, Liu H Y, Tang F Q. *Adv Mater*, 2010, 22: 4885
- [24] Zhu G R, Yang Q H, Jiang D M, Yang J, Zhang L, Li Y, Li C. *J Chromatogr A*, 2006, 1103: 257
- [25] Shi Y F, Li B, Wang P, Dua R, Zhao D Y. *Microporous Mesoporous Mater*, 2012, 155: 252.
- [26] Wang P, Shi Q H, Shi Y F, Clark K K, Stucky G D, Keller A A. *J Am Chem Soc*, 2009, 131: 182
- [27] Lin K F, Wang L F, Meng F Y, Sun Zh H, Yang Q, Cui Y M, Jiang D Zh, Xiao F Sh. *J Catal*, 2005, 235: 423
- [28] Inumaru K, Ishihara T, Kamiya Y, Okuhara T, Yamanaka S. *Angew Chem, Int Ed*, 2007, 46: 7625
- [29] Hamilton C E, Lomeda J R, Sun Zh Z, Tour j M, Barron A R. *Nano Res*, 2010, 3: 138
- [30] Li Y Y, Kong N, Lin J J, Duan S P, Chen W, Tian S Y, Wang X B. *Chin J Appl Chem* (李远耀, 孔妮, 林晶晶, 段世鹏, 陈伟, 田思瑶, 王贤保. 应用化学), 2012, 29: 251
- [31] Stöber W, Fink A, Bohn E. *J Colloid Interf Sci*, 1968, 26: 62
- [32] Chen Zh, Cui Zh M, Niu F, Jiang L, Song W G. *Chem Commun*, 2010, 46: 6524
- [33] Lan Y, Zhang M Ch, Zhang W Q, Yang L. *Chem Eur J*, 2009, 15: 3670
- [34] Zhang Y P, Xu Y, Liao S J, Shen Q. *Chin J Catal* (张一平, 徐筠, 廖世健, 沈琪. 催化学报), 1990, 11: 224
- [35] Qiu K, Zhang Q, Jiang T, Ma L L, Wang T J, Zhang X H, Qiu M H. *Chin J Catal* (邱珂, 章青, 江婷, 马隆隆, 王铁军, 张兴华, 丘明煌. 催化学报), 2011, 32: 612

## 氟功能化蛋黄型氧化硅材料负载Pd纳米粒子用于水相烯烃加氢

李晓菲<sup>a,b</sup>, 张文娟<sup>b</sup>, 张丽敏<sup>a,\*</sup>, 杨恒权<sup>b,#</sup>

<sup>a</sup>山西师范大学材料与化学学院, 山西临汾041000

<sup>b</sup>山西大学化学化工学院, 山西太原030006

**摘要:** 先将Pd纳米粒子负载于SiO<sub>2</sub>球表面上, 再经包裹、刻蚀、硅烷化修饰, 得到氟丙基功能化“蛋黄”型结构催化剂. 并采用X射线衍射、透射电镜、N<sub>2</sub>吸附-脱附和热重等对催化剂进行了表征. 结果表明, 该催化剂在水相烯烃加氢反应中表现出较高的活性, 明显高于未经氟丙基修饰的同类催化剂. 该催化剂通过离心便可实现回收, 多次循环使用后仍保持较高的活性.

**关键词:** 钯; 功能化; 烯烃; 水相; 加氢

收稿日期: 2012-12-24. 接受日期: 2013-03-05. 出版日期: 2013-06-20.

\*通讯联系人. 电话: 13663578554; 电子信箱: zhangliminsxnu@gmail.com

#通讯联系人. 电话: 13643472170; 电子信箱: hqyang@sxu.edu.cn

基金来源: 国家自然科学基金(20903065, 21173137).

本文的英文电子版由Elsevier出版社在ScienceDirect上出版(<http://www.sciencedirect.com/science/journal/18722067>).

### 1. 前言

水是一种廉价、安全、无污染的绿色环保型溶剂, 近

年来以水为介质的催化反应引起了人们极大的兴趣<sup>[1-6]</sup>. 然而, 大多数有机反应物与水互不相溶, 不利于反应物与催化剂的充分接触, 导致水相催化反应速率普遍较低.

为了提高反应速率,通常情况下需加入表面活性剂或共溶剂<sup>[7,8]</sup>,但给产品分离和纯化带来了困难.因此,研发用于水相中有机反应的高效催化剂是一项富有挑战性的课题.

“蛋黄”(yolk-shell)型介孔材料是近年来发现的一种新型催化材料<sup>[9–20]</sup>,由于具有独特的结构,而成为催化领域的研究热点.与介孔材料MCM-41和SBA-15相比,该材料具有独特的中空结构,密度小,有利于催化剂悬浮于水中.而且中空结构和介孔壳层能使反应物分子很快扩散到催化剂周围,从而大幅度提高催化反应的速率<sup>[21,22]</sup>.与传统核壳结构类材料相比,“蛋黄”类材料的外壳与内核间存在空腔结构,可富集并容纳更多的反应物分子,有利于反应物和催化剂充分接触.此外,其介孔壳能够对负载在壳内的金属纳米粒子起到保护作用,同时可提高催化剂的稳定性<sup>[23]</sup>.

对于水相催化反应,增加催化剂表面的疏水性有利于提高催化剂的稳定性和活性. Yang课题组<sup>[24]</sup>研究表明,经有机官能团修饰的介孔材料水热稳定性显著提高. Shi等<sup>[25,26]</sup>发现,疏水化修饰能提高材料对水中有机污染物的吸附能力. Lin等<sup>[27]</sup>也证明疏水性基团的引入可提高水相催化反应速率. Inumaru等<sup>[28]</sup>发现,限阈在疏水性微环境中的杂多酸表现出超高的催化活性.由此可见,疏水化修饰的催化剂能有效吸附反应物分子,从而显著提高反应速率.但是,催化剂疏水性过强不利于与反应物接触,使得催化剂活性降低.氟丙基是一种中等疏水性官能团,用它修饰过的催化剂具有适中的疏水性<sup>[29,30]</sup>,能提高催化反应速率.然而,氟丙基功能化的“黄蛋”结构催化剂的制备及其在水相中有机反应的应用鲜见报道.

本文先通过浸渍、还原将Pd负载于SiO<sub>2</sub>上,然后在碱性条件下通过包裹、刻蚀得到“蛋黄”型氧化硅球(yPd@mSiO<sub>2</sub>),最后将氟丙基嫁接到材料上,制备得到功能化“蛋黄”型催化剂(yPd@mSiO<sub>2</sub>-F),并采用X射线衍射、透射电镜、N<sub>2</sub>吸附-脱附和热重等技术对样品的结构和组成等进行了表征,通过水相加氢反应考察其催化活性及循环使用性能.

## 2. 实验部分

### 2.1. 催化剂的制备

在500 ml的烧瓶中加入200 ml无水乙醇(AR,天津富宇试剂公司)、16 ml氨水(AR,阿拉丁试剂公司)、12.2 ml去离子水,室温下搅拌30 min后,再加入12.4 ml正硅

酸乙酯(TEOS, AR,阿拉丁试剂公司),继续搅拌12 h,经抽滤、去离子水反复洗涤至pH为中性后烘干,即得到SiO<sub>2</sub><sup>[31]</sup>.

称取0.8 g所制SiO<sub>2</sub>材料于试管中,加入10 ml乙酸钯的甲苯溶液(含乙酸钯8.4 mg),室温下搅拌4 h,离心取走上清液后,加入16 ml的甲苯-乙醇混合液(V<sub>甲苯</sub>:V<sub>乙醇</sub> = 20:1)和适量的NaBH<sub>4</sub>(阿拉丁试剂公司),于室温还原4 h,然后离心分离得到固体,用乙醇洗涤4次,真空干燥,即得到Pd/SiO<sub>2</sub>.

将0.6 g所制Pd/SiO<sub>2</sub>样品和120 ml去离子水加到200 ml圆底烧瓶中,超声15 min,缓慢加到由0.9 g十六烷基三甲基溴化铵(CTAB,阿拉丁试剂公司)、180 ml无水乙醇、180 ml去离子水、3.3 ml氨水组成的混合液中,于室温搅拌30 min后,加入1.0575 g的TEOS,继续搅拌10 h,经抽滤、烘干后,将其转到250 ml烧瓶中,加入120 ml去离子水超声至分散均匀,再加入2.544 g的Na<sub>2</sub>CO<sub>3</sub>(AR,天津风船试剂公司),在N<sub>2</sub>保护下于50 °C搅拌12 h对其进行刻蚀.最后,抽干后经硝酸铵乙醇溶液萃取,即得到yPd@mSiO<sub>2</sub>.

称取0.5 g的yPd@mSiO<sub>2</sub>样品于试管中,加入5 ml含0.1635 g (0.75 mmol)三氟丙基三甲氧基硅烷(AR,阿拉丁试剂公司)的甲苯,在N<sub>2</sub>保护下于100 °C回流4 h,然后离心分离,所得固体用甲苯和乙醇充分洗涤,抽干,即得到yPd@mSiO<sub>2</sub>-F.

### 2.2. 催化剂的表征

采用日本JEOL JEM-2000EX型TEM进行形貌观测,加速电压120 kV.在液氮温度(-196 °C)下,以N<sub>2</sub>为吸附质在美国Micromeritics公司ASAP2020型物理吸附仪上表征材料的比表面积.采用X射线衍射仪(D/max-2400日本理学)进行物相和结构分析,Cu K<sub>α</sub>射线源,管电压40 kV,管电流100 mA,扫描速率5°/min,扫描角度分辨率0.02°.采用热重分析仪(NETZSCH TG,德国)对材料的组成进行分析,N<sub>2</sub>气氛,以25°/min由室温升至900 °C.

### 2.3. 烯烃加氢反应

烯烃加氢反应在配有水浴、热电偶以及磁力搅拌器的三口圆底烧瓶中进行.将6 ml的H<sub>2</sub>O,1 mmol烯烃反应底物以及制备好的催化剂(0.1 mol%)加入反应器中.通入氢气置换出反应器中的空气后,将压力升至0.15 MPa.开启搅拌器(转速为500 r/min),加热至反应温度开始反应.反应结束后,离心分离出催化剂.反应产物采用美国Agilent 7890A型气相色谱分析仪分析,FID检测器.



### 3. 结果与讨论

#### 3.1. 催化剂制备过程与表征结果

yPd@mSiO<sub>2</sub>的制备过程分为四步(见图1). 为了将Pd纳米粒子固载于“蛋黄”材料内部, 先通过浸渍、还原将Pd纳米粒子负载于SiO<sub>2</sub>球上, 在CTAB存在下在其表面上生长一层SiO<sub>2</sub>壳, 然后在碱性条件下用Na<sub>2</sub>CO<sub>3</sub>对SiO<sub>2</sub>内核进行刻蚀, 最后通过溶剂萃取去除模板剂即得到“蛋黄”型结构催化剂. 与采用高温焙烧去除碳球得到中空结构的方法<sup>[32]</sup>相比, 该方法制备条件温和, 避免了因高温焙烧引起的结构塌陷及催化活性组分失活.

图2为每一步合成样品的N<sub>2</sub>吸附-脱附等温曲线, 相应织构参数列于表1. 可以看出, SiO<sub>2</sub>球的比表面积仅为18 m<sup>2</sup>/g, 孔体积为0.06 cm<sup>3</sup>/g. Pd/SiO<sub>2</sub>经SiO<sub>2</sub>包裹得到Pd/SiO<sub>2</sub>@mSiO<sub>2</sub>, 其吸附曲线为IV型, 在相对压力0.1~0.3间出现毛细管凝聚现象; 其吸附量明显增大, 比表面积和孔体积分别增至408 m<sup>2</sup>/g和0.23 cm<sup>3</sup>/g, 这是由于CTAB存在下, Pd/SiO<sub>2</sub>表面形成了SiO<sub>2</sub>孔道结构. 经刻蚀得到yPd@mSiO<sub>2</sub>的吸附的吸附等温线也表现为典型的IV型, 在相对压力0.3~0.5间出现了毛细管凝聚现象, 表明具有介孔结构; 且yPd@mSiO<sub>2</sub>在相对压力0.5~1.0范围内的吸附分支和脱附分支没有重合, 出现明显的H4型滞后环, 证明该材料具有中空结构. 与Pd/SiO<sub>2</sub>@mSiO<sub>2</sub>相比, yPd@mSiO<sub>2</sub>的比表面积和孔体积显著增加, 分别高达841 m<sup>2</sup>/g和1.01 cm<sup>3</sup>/g. 这主要是由于yPd@mSiO<sub>2</sub>的SiO<sub>2</sub>内核被刻蚀掉, 模板剂也得以充分的去除. 经氟丙基修饰后, 所得yPd@mSiO<sub>2</sub>-F样品吸附曲线类型未发生改变, 但其比表面积、孔体积和孔径都明显减小, 表明氟丙基成功引入到yPd@mSiO<sub>2</sub>材料上.

图3是SiO<sub>2</sub>, Pd/SiO<sub>2</sub>和yPd@mSiO<sub>2</sub>的TEM照片. 由图可见, 所合成的SiO<sub>2</sub>由大小均匀、高分散的小球组成, 其直径在200 nm左右; 将Pd纳米粒子负载到SiO<sub>2</sub>表面上得到的Pd/SiO<sub>2</sub>样品中Pd粒子的大小基本均匀, 尺寸为4~10 nm; 经包裹、刻蚀得到的yPd@mSiO<sub>2</sub>材料由许多小球颗粒组成, 其大小相对均匀, 尺寸在500 nm左右. 与SiO<sub>2</sub>球相比, yPd@mSiO<sub>2</sub>微球的尺寸明显增大; 大多数小球颗粒由内核与外壳组成, 且两者之间存在空腔, 与图2一致. 图4为yPd@mSiO<sub>2</sub>和yPd@mSiO<sub>2</sub>-F的XRD谱. 由图可见, yPd@mSiO<sub>2</sub>在2 $\theta$   $\approx$  2.3°处出现了较强的衍射峰, 进一步证明所合成的“蛋黄”型氧化硅球外壳具有介孔结构. 氟丙基修饰后, 材料在2 $\theta$   $\approx$  2.3°处依然有衍射峰, 且峰强度基本保持不变, 说明氟丙基的引入并未破坏材料的有序结构.

图5是yPd@mSiO<sub>2</sub>和yPd@mSiO<sub>2</sub>-F的TG曲线. 由图可见, 在室温~900 °C, Pd@mSiO<sub>2</sub>存在三个失重峰: 低于200 °C时, 样品失重3.48%, 可归属于材料表面物理吸附的水; 200~320 °C失重4.4%, 这是由少量表面活性剂的分解所致; 在320~650 °C样品失重3.54%, 主要是由硅羟基高温缩合脱水造成. Pd@mSiO<sub>2</sub>-F样品失重也分为三个阶段: 低于200 °C失重1.17%, 明显低于Pd@mSiO<sub>2</sub>, 这是由于氟丙基的引入使材料表面的疏水性增强, 吸附水的量减少; 在200~320 °C间失重3.16%, 这也是因少量表面活性剂的分解所致; 在320~650 °C失重高达15.31%, 主要是由共价键连接的氟丙基的分解和少量硅羟基在高温条件下缩合脱水造成. 经比较, 可估算出氟丙基的负载量为1.2 mmol/g, 与元素分析结果基本吻合.

#### 3.2. 催化剂的活性

烯烃加氢反应在精细化学品合成中有着广泛的应用, 许多学者正在寻求水相反应的高效催化剂, 并取得了可喜的进展<sup>[33–35]</sup>. 因此, 本文选择水相加氢反应来评价新型“蛋黄”型核壳结构催化剂的性能. 将催化剂yPd@mSiO<sub>2</sub>-F和yPd@mSiO<sub>2</sub>用于丙烯酸甲酯加氢反应中, 通过跟踪H<sub>2</sub>压降来比较反应速率, 结果示于图6. 可以看出, 相同的反应条件下, yPd@mSiO<sub>2</sub>-F的耗氢速率明显大于yPd@mSiO<sub>2</sub>, 表明前者催化活性更高. 如图7所示, 两种催化剂上甲基丙烯酸乙酯的压降均随时间延长而下降, 但yPd@mSiO<sub>2</sub>-F的压降速度明显更快, 与图6结果一致. 由此可见, yPd@mSiO<sub>2</sub>-F具有更高的催化活性.

为了进一步考察催化剂的性能, 将yPd@mSiO<sub>2</sub>和yPd@mSiO<sub>2</sub>-F用于其它烯烃加氢反应中, 结果示于表2. 可以看出, 以苯乙烯为底物, 反应45 min, yPd@mSiO<sub>2</sub>和yPd@mSiO<sub>2</sub>-F上苯乙烯转化率分别是45%和88%. 对于脂肪类烯烃, 如丙烯酸丁酯、丙烯酸甲酯、甲基丙烯酸丁酯等, 在相同反应条件下, yPd@mSiO<sub>2</sub>-F上底物的转化率明显高于yPd@mSiO<sub>2</sub>. 以丙烯酰胺为底物, 反应60 min时, yPd@mSiO<sub>2</sub>对应的转化率是49%, yPd@mSiO<sub>2</sub>-F对应的转化率是99%, 后者是前者的2倍. 综上所述, 在水相烯烃加氢反应中, yPd@mSiO<sub>2</sub>-F的催化活性明显高于yPd@mSiO<sub>2</sub>. 这是由于yPd@mSiO<sub>2</sub>的壳层经氟丙基修饰后具有中等程度的疏水性, 有利于将水相中低浓度的有机反应物富集到“蛋黄”型材料的腔内, 使反应物和Pd金属粒子充分接触, 进而提高催化反应速率.

#### 3.3. 催化剂的循环使用性能

在纯水介质中, 以丙烯酸丁酯加氢反应来评价



yPd@mSiO<sub>2</sub>-F催化剂的循环使用性能,结果列于表3.可以看出,第一次使用时反应90 min底物转化率为99%.反应结束后,通过离心、洗涤回收催化剂,真空干燥后直接加入底物用于第二次反应,反应相同时间底物转化率仍可达99%.使用至第五次底物转化率仍可达99%.由此可见,yPd@mSiO<sub>2</sub>-F具有良好的循环使用性能,且该催化剂易回收.

为了验证在反应过程中yPd@mSiO<sub>2</sub>-F催化剂上的活性组分Pd纳米粒子是否流失,我们对滤液进行了实验.按表2实验4的条件,反应30 min后停止,经高速离心后得到滤液,测得丙烯酰胺的转化率达52%;然后,相同条件下继续反应30 min,底物转化率没有明显的增加(54%),远低于相同时间内在催化剂存在下99%的转化率(见表2,实验4),说明在反应过程中对转化率的贡献来源于催化剂上的活性组分,而不是滤液中流失的Pd纳米粒子.这表明“蛋黄”型结构能有效阻止Pd纳米粒子的流失.为了进一步验证催化剂的稳定性,我们测得循环使用5次

后的yPd@mSiO<sub>2</sub>-F样品的比表面积和孔体积分别为382 m<sup>2</sup>/g和0.45 cm<sup>3</sup>/g;与新鲜的催化剂相比稍有所降低,证明该催化剂具有良好的水热稳定性.

#### 4. 结论

通过包裹、刻蚀、硅烷化修饰成功地将Pd负载于“蛋黄”型氧化硅材料内,得到了氟丙基功能化的“蛋黄”型结构催化剂.结果显示,该催化剂比表面积较大,壳层外具有均匀分布的介孔孔道.在水相烯烃加氢反应中yPd@mSiO<sub>2</sub>-F的活性高于yPd@mSiO<sub>2</sub>.这可能是由于yPd@mSiO<sub>2</sub>的壳层经氟丙基修饰后具有中等程度的疏水性,有利于将水相中低浓度的有机反应物富集到“蛋黄”型材料的腔内,使反应物和Pd金属粒子充分接触,进而提高催化反应速率.yPd@mSiO<sub>2</sub>-F循环使用5次后活性没有降低,表明其具有良好的稳定性.独特的结构和易功能化的特点使“蛋黄”型结构催化剂在水相反应中具有有良好的应用前景.